Chakrabarti, Saikat and Kyriakides, Elias (2009) ***PMU measurement uncertainty considerations in WLS state estimation.*** Transactions on Power Systems, 24(2). pp. 1062-1071.

PMU Measurement Uncertainty Considerations in WLS State Estimation

Saikat Chakrabarti, *Member, IEEE*, and Elias Kyriakides, *Member, IEEE*

***Abstract*—A method to assign weights to the measurements obtained through phasor measurement units (PMUs) in a weighted least squares (WLS) state estimation is presented in this paper. The uncertainties for direct measurements are obtained from the manufacturer's specifications. For pseudo-measurements, the uncertainties are evaluated by using the classical uncertainty propagation theory. The propagation of measurement uncertainty as a function of line length and conductor type is also investigated. The lower and upper bounds of the estimated states considering the measurement uncertainties are found by using linear programming. The proposed method is applied on the IEEE 14-, 30-, 57-, and 118-bus test systems, and the state estimation results including the lower and upper bounds of the estimated states are presented.**

***Index Terms*—Measurement uncertainty, phasor measurement units, state estimation, total vector error.**

I. Introduction

MODERN-DAY power systems are being operated under heavily stressed conditions to cater for the rapidly growing demand for electricity, and to maintain an economic operation under a highly competitive deregulated environment. A wide area monitoring, protection, and control (WAMPAC) system is therefore becoming increasingly essential for improved power system planning, operation, maintenance, and energy trading [1]. Phasor measurement units (PMUs), utilizing synchronized measurement technology (SMT), are vital elements of a WAMPAC. A PMU, when placed at a bus, can measure the voltage phasor at the bus, as well as the current phasors through the lines incident to the bus. It samples the ac voltage and current waveforms while synchronizing the sampling instants with a global positioning system (GPS) clock. The computed values of voltage and current phasors are then time-stamped and transmitted by the PMUs to the local or remote receiver [2].

The measurements provided by PMUs are usually superior to the conventional measurements in a power system in terms of resolution and accuracy. However, these measurements are not free from errors. To determine the confidence levels that can be assigned to the PMU measurements, it is therefore important to evaluate the uncertainties associated with the PMU measurements. This paper presents a methodology to evaluate the uncertainties associated with the states measured or computed by a PMU. A methodology to assign weights to the PMU measurements in the weighted least squares (WLS) state estimation is also proposed in this paper.

The major sources of uncertainties in the measurements by the PMUs are due to the instrument transformers, the A/D converters, and the cables connecting them [3]. The uncertainties due to the instrument transformers and the cables are mostly systematic and predictable in nature [3]. Many of the PMUs available in the market are featured with the option of external calibration, which can be used to compensate for the uncertainties due to these two sources. However, the uncertainties due to the A/D converter and the associated computational algorithm are difficult to compensate, and may bias the PMU measurements. The required accuracy of the PMU measurements and the methods of verifying compliance with various performance metrics are described in [4] and [5]. The problem of finding optimal PMU locations for power system state estimation is well investigated in the literature [6]–[13]. However, the propagation of PMU measurement uncertainty along the transmission lines, and consequently the uncertainties in the estimated states is not adequately addressed so far. References [14] and [15] describe the use of two approaches: classical uncertainty propagation theory, and the random fuzzy variables, to compute the PMU measurement uncertainties. This paper uses a distributed parameter model of the transmission lines to obtain more accurate expressions for the uncertainties associated with the PMU measurements. Analysis of the uncertainties in the estimated states of a power system is discussed in [16] and [17]. The present paper extends the method proposed in [16] and [17] to evaluate the uncertainties in the final estimated states based on PMU measurements. Errors due to transmission line parameters are also neglected.

The paper is organized as follows. The methodology to compute the uncertainties associated with the PMU measurements is described in Section II. Section III briefly discusses the state estimation process using PMU measurements. The method to compute the uncertainties in the final estimated states is given in Section IV. The case studies are presented in Section V, and Section VI concludes the paper.

II. Measurement Uncertainty Calculations

The PMUs, when placed at a bus, can measure the voltage phasor at that bus, as well as the current phasors on the incident lines. It is therefore possible to compute the voltage phasor at the other end of the lines through the known parameters of the

Manuscript received July 01, 2008; revised November 11, 2008. First published March 21, 2009; current version published April 22, 2009. This work was supported in part by the Cyprus Research Promotion Foundation under grant ΠΔΕ/0505/06. Paper no. TPWRS-00514-2008.

S. Chakrabarti is with the School of Engineering Systems, Queensland University of Technology, Brisbane, Australia (e-mail: saikat.chakrabarti@gmail.com).

E. Kyriakides is with the KIOS Research Center for Intelligent Systems and Networks and the Department of Electrical and Computer Engineering, University of Cyprus, Nicosia, Cyprus (e-mail: elias@ucy.ac.cy).

Color versions of one or more of the figures in this paper are available online at http://ieeexplore.ieee.org.

Digital Object Identifier 10.1109/TPWRS.2009.2016295

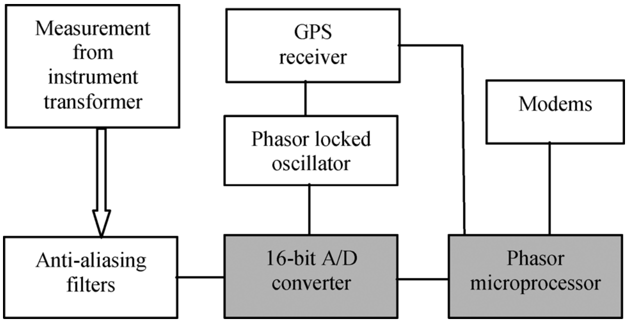

Fig. 1. Basic block diagram of a PMU highlighting the considered sources of uncertainty [2].

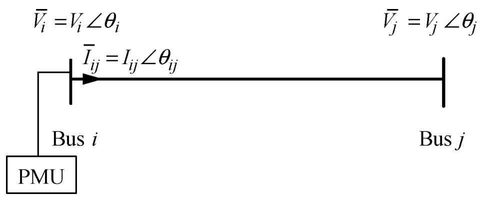

Fig. 2. Two-bus system having PMU at one end.

transmission lines [12], [13]. It is assumed that a PMU has sufficient number of channels to measure the current phasors through all lines incident to the bus where it is placed. The uncertainties in the angles and magnitudes of the voltage phasors measured or computed by the PMU as a result of the uncertainties in the A/D converter and the associated computational logic are considered in this paper. Fig. 1 shows the basic block diagram of a PMU, highlighting the considered sources of measurement uncertainty [2].

The computation of the voltage phasor at a bus, which is connected to a bus with an installed PMU can be illustrated with the help of the two-bus system shown in Fig. 2. Let there be a PMU installed at bus i, which measures the voltage phasor $\overline{V}_i = V_i \angle \theta_i$ at bus i and the current phasor $\overline{I}_{ij} = I_{ij} \angle \theta_{ij}$ through the line connected to bus j.

The voltage at bus j can be expressed as [18]

$$\overline{V}_j = \left(\frac{\overline{V}_i - \overline{I}_{ij} \overline{Z}_c}{2} \right) e^{\overline{\gamma} l} + \left(\frac{\overline{V}_i + \overline{I}_{ij} \overline{Z}_c}{2} \right) e^{-\overline{\gamma} l}. \quad (1)$$

Here $\overline{\gamma} = \sqrt{zy} = (\gamma_r + j\gamma_i)$ is the propagation constant and $\overline{Z}_c = \sqrt{z/y} = Z_c \angle \theta_z$ is the characteristic impedance of the line; z and y are the series impedance and shunt admittance of the line per unit length, respectively; and l is the length of the transmission line between buses i and j. The distributed parameter model of the transmission line is used in this work to achieve greater accuracy in the computation of the uncertainties in PMU measurements. Using (1), $\overline{V}_j$ can be expressed in the following complex form:

$$\overline{V}_j = A + jB \quad (2)$$

where

$$A = \left[V_i (e^{\gamma_r l} \cos \varphi_1 + e^{-\gamma_r l} \cos \varphi_2) - I_{ij} Z_c (e^{\gamma_r l} \cos \varphi_3 - e^{-\gamma_r l} \cos \varphi_4) \right] / 2 \quad (3)$$

$$B = \left[V_i (e^{\gamma_r l} \sin \varphi_1 + e^{-\gamma_r l} \sin \varphi_2) - I_{ij} Z_c (e^{\gamma_r l} \sin \varphi_3 - e^{-\gamma_r l} \sin \varphi_4) \right] / 2 \quad (4)$$

$$\left. \begin{array}{l} \varphi_1 = \theta_i + \gamma_i l; \varphi_2 = \theta_i - \gamma_i l \\ \varphi_3 = \theta_{ij} + \theta_z + \gamma_i l; \varphi_4 = \theta_{ij} + \theta_z - \gamma_i l \end{array} \right\}. \quad (5)$$

The magnitude V_j and the phase angle θ_j of the voltage phasor $\overline{V}_j$ are given by

$$V_j = \sqrt{A^2 + B^2} \quad (6)$$

$$\theta_j = \tan^{-1}(B/A). \quad (7)$$

From (1)–(7), it is evident that the magnitude and the phase angle of the voltage phasor $\overline{V}_j$ are functions of the magnitudes and phase angles of the voltage and current phasors measured by the PMU at bus i. Equations (6) and (7) therefore can be expressed as

$$V_j = f_{V_j}(V_i, \theta_i, I_{ij}, \theta_{ij}) \quad (8)$$

$$\theta_j = f_{\theta_j}(V_i, \theta_i, I_{ij}, \theta_{ij}). \quad (9)$$

Using (3)–(9), the following partial derivatives can be computed, which are required to compute the combined uncertainty in the measurement of the voltage magnitude and the phase angle at bus j [18]:

$$\frac{\partial V_j}{\partial V_i} = \left[e^{\gamma_r l} (A \cos \varphi_1 + B \sin \varphi_1) + e^{-\gamma_r l} (A \cos \varphi_2 + B \sin \varphi_2) \right] / [2\sqrt{A^2 + B^2}] \quad (10)$$

$$\frac{\partial V_j}{\partial \theta_i} = -V_i \left[e^{\gamma_r l} (A \sin \varphi_1 - B \cos \varphi_1) + e^{-\gamma_r l} (A \sin \varphi_2 - B \cos \varphi_2) \right] / [2\sqrt{A^2 + B^2}] \quad (11)$$

$$\frac{\partial V_j}{\partial I_{ij}} = -Z_c \left[e^{\gamma_r l} (A \cos \varphi_3 + B \sin \varphi_3) - e^{-\gamma_r l} (A \cos \varphi_4 + B \sin \varphi_4) \right] / [2\sqrt{A^2 + B^2}] \quad (12)$$

$$\frac{\partial V_j}{\partial \theta_{ij}} = I_{ij} Z_c \left[e^{\gamma_r l} (A \sin \varphi_3 - B \cos \varphi_3) - e^{-\gamma_r l} (A \sin \varphi_4 - B \cos \varphi_4) \right] / [2\sqrt{A^2 + B^2}] \quad (13)$$

$$\frac{\partial \theta_j}{\partial V_i} = \left[e^{\gamma_r l} (A \sin \varphi_1 - B \cos \varphi_1) + e^{-\gamma_r l} (A \sin \varphi_2 - B \cos \varphi_2) \right] / \left[2(A^2 + B^2) \right] \quad (14)$$

$$\frac{\partial \theta_j}{\partial \theta_i} = V_i \left[e^{\gamma_r l} (A \cos \varphi_1 + B \sin \varphi_1) + e^{-\gamma_r l} (A \cos \varphi_2 + B \sin \varphi_2) \right] / \left[2(A^2 + B^2) \right] \quad (15)$$

$$\frac{\partial \theta_j}{\partial I_{ij}} = -Z_c \left[e^{\gamma_r l} (A \sin \varphi_3 - B \cos \varphi_3) - e^{-\gamma_r l} (A \sin \varphi_4 - B \cos \varphi_4) \right] / \left[2(A^2 + B^2) \right] \quad (16)$$

$$\frac{\partial \theta_j}{\partial \theta_{ij}} = -I_{ij} Z_c \left[e^{\gamma_r l}(A\cos\varphi_3 + B\sin\varphi_3) - e^{-\gamma_r l}(A\cos\varphi_4 + B\sin\varphi_4) \right] / \left[2(A^2+B^2)\right]. \quad (17)$$

As mentioned in the beginning of this section, the PMUs considered in this work have multiple measurement channels. It is assumed that all channels are independent, and therefore there is zero correlation among the quantities measured by the PMU. By using classical uncertainty propagation theory, the combined standard uncertainty in the voltage magnitude V_j and the phase angle θ_j can be given by [19]

$$u(V_j) = \sqrt{\sum_{k=1}^{4} \left[\partial V_j / \partial \mathbf{p}(k)\right]^2 \left[u\left(\mathbf{p}(k)\right)\right]^2} \quad (18)$$

$$u(\theta_j) = \sqrt{\sum_{k=1}^{4} \left[\partial \theta_j / \partial \mathbf{p}(k)\right]^2 \left[u\left(\mathbf{p}(k)\right)\right]^2} \quad (19)$$

where $\mathbf{p} = [V_i, \theta_i, I_{ij}, \theta_{ij}]$, and $u(\mathbf{p}(k))$ is the standard uncertainty in the measurement $\mathbf{p}(k)$.

To evaluate the combined standard uncertainties in (18) and (19), one needs to know the standard uncertainties in the voltage and current magnitude and phase angle measurements by the PMU. Usually, the maximum measurement uncertainty is specified by PMU manufacturers [20]. In the absence of any probability distribution of the measurement uncertainty specified by the manufacturer, a uniform distribution may be assumed. The standard uncertainty in the measurement can then be expressed in terms of the maximum measurement uncertainty as shown in the following[19]:

$$u\left(\mathbf{p}(k)\right) = \frac{\Delta \mathbf{p}(k)}{\sqrt{3}} \quad (20)$$

where $\Delta \mathbf{p}(k)$ is the maximum manufacturer-specified uncertainty in the measurement of $\mathbf{p}(k)$.

The standard uncertainties associated with the PMU measurements are used in the next section to provide a basis for weighing measurements from different PMUs while estimating the states of the power system. When a PMU is placed at a bus, the standard uncertainties in the voltage magnitude and phase angle are computed directly by using (20). For other buses, where the voltage phasors are computed by using the current measurement through the connecting lines, the standard uncertainties in measurements are computed by using (18) and (19).

The desirable accuracy of the PMUs in the measurement of voltage or current phasors is often specified in terms of total vector error (TVE), which is defined as [4], [5]

$$\text{TVE} = \frac{|\overline{X}_{\text{measured}} - \overline{X}_{\text{theoretical}}|}{|\overline{X}_{\text{theoretical}}|} \quad (21)$$

where $\overline{X}_{\text{measured}}$ is the phasor measured by the PMU; $\overline{X}_{\text{theoretical}}$ is the theoretical or ideal value of the phasor.

Normally, TVE is expressed as a percentage of the magnitude of the theoretical value of the phasor, and a TVE of 1% is commonly used at different compliance levels specified for PMU performance [4]. The maximum values of the TVEs for the voltage phasor measurement can be obtained by solving the following set of nonlinear optimization problems:

$$\text{Maximize} \left(\frac{|\overline{V}_{i,\text{measured}} - \overline{V}_{i,\text{theoretical}}|}{|\overline{V}_{i,\text{theoretical}}|} \right) \quad \forall i = 1, \ldots, m \quad (22)$$

$$\text{subject to } \mathbf{z}_{\text{lower}} \leq \mathbf{z} \leq \mathbf{z}_{\text{upper}} \quad (23)$$

where $\overline{V}_{i,\text{measured}}$ and $\overline{V}_{i,\text{theoretical}}$ are the measured and theoretical values of the voltage phasor at bus i, respectively; $\mathbf{z}_{\text{lower}}$ and $\mathbf{z}_{\text{upper}}$ are the vectors containing the lower and upper bounds of the measurements, and are defined as follows:

$$\mathbf{z}_{\text{lower}} = \mathbf{z} - [\Delta z_1, \Delta z_2, \ldots, \Delta z_m]^{\text{T}} \quad (24)$$

$$\mathbf{z}_{\text{upper}} = \mathbf{z} + [\Delta z_1, \Delta z_2, \ldots, \Delta z_m]^{\text{T}} \quad (25)$$

where Δz_i is the maximum uncertainty corresponding to the ith measurement. The value of Δz_i is obtained from manufacturer's specifications for direct measurements, and by using (18) and (19) for pseudo-measurements.

III. State Estimation Using PMU Measurements

The number of actual or pseudo-measurements obtained in a power system are usually more than the number of states to be estimated, so as to ensure greater reliability in the estimated states and better quality in terms of estimation accuracy through this redundancy in the measurements. A WLS estimator can be used to obtain the states of the power system, based on the available measurements from the PMUs. When only PMU measurements are present in the system, as assumed in the present study, the set of measurement equations is linear and can be expressed by [21]

$$\mathbf{z} = \mathbf{A}\mathbf{x} + \mathbf{e} \quad (26)$$

where $\mathbf{z} = [z_1, z_2, \ldots, z_m]^{\text{T}}$ is the measurement vector containing the bus voltage magnitudes and angles measured or computed by the PMUs; $\mathbf{x} = [x_1, x_2, \ldots, x_n]^{\text{T}}$ is the vector of states for the power system, i.e., the vector of bus voltage magnitudes and phase angles; $\mathbf{A}$ is the matrix relating the measurements to the states; and $\mathbf{e} = [e_1, e_2, \ldots, e_m]^{\text{T}}$ is the vector of measurement uncertainties. The measurement uncertainties are commonly assumed to have the following statistical properties [21].

1) The measurement uncertainties have a zero mean, i.e.,

$$\text{E}(e_i) = 0, \quad \forall i = 1, \ldots, m \quad (27)$$

where $\text{E}(e_i)$ is the expectation of e_i.

2) The measurement uncertainties are independent, i.e.,

$$\text{E}(e_i e_j) = 0, \ \forall i = 1, \ldots, m; j = 1, \ldots, m; i \neq j. \quad (28)$$

Hence, the covariance of $\mathbf{e}$ is given by

$$\mathrm{Cov}(\mathbf{e})=\mathrm{E}(\mathbf{e}.\mathbf{e}^{\mathrm{T}})=\mathbf{R}=\mathrm{diag}\left\{u^2(z_1),u^2(z_2),\ldots,u^2(z_m)\right\} \tag{29}$$

where $\mathbf{R}$ is the measurement uncertainty covariance matrix that provides the basis for weighing the PMU measurements; $u(z_i)$ is the standard uncertainty in the ith measurement.

The WLS estimated states are given by [21], [22]

$$\hat{\mathbf{x}}=(\mathbf{A}^{\mathrm{T}}\mathbf{R}^{-1}\mathbf{A})^{-1}\mathbf{A}^{\mathrm{T}}\mathbf{R}^{-1}\mathbf{z}=\mathbf{M}\mathbf{z} \tag{30}$$

where $\mathbf{M}=\left(\mathbf{A}^{\mathrm{T}}\mathbf{R}^{-1}\mathbf{A}\right)^{-1}\mathbf{A}^{\mathrm{T}}\mathbf{R}^{-1}$ is the matrix converting the measurements to the estimated states. As long as the system topology does not change, the matrix $\mathbf{M}$ remains constant [22]. Using (30), the states can be estimated directly by using the PMU measurements, without requiring any iteration.

It is possible to include PMU measurements of currents in the WLS state estimation process, as is done with conventional current measurements [21]. This will lead to nonlinear measurement functions, and consequently, an iterative procedure will be needed to obtain the estimates of the states. In any case, this is not a problem as the synchronized measurements will be combined with conventional measurements in an actual estimator, resulting in an iterative estimator. Section V describes a method to compute the uncertainties in the estimated states in the presence of both synchronized and conventional measurements.

A common practice in weighing PMU measurements in a WLS state estimation is assigning weights proportional to the inverse of the variance in the corresponding PMU measurement uncertainty [23]. While the same approach is followed in this work to assign weights to the direct measurement of voltage magnitude and phase angles by the PMUs, the weights assigned to the pseudo-measurements are based on the computed values of the standard uncertainties. For example, for the two-bus system shown in Fig. 2, the weights assigned to the voltage magnitude and phase angle measurement at bus i are proportional to $u^{-2}(V_i)$ and $u^{-2}(\theta_i)$, which are directly computed from the manufacturer's data sheets by using (20). The corresponding weights for the computed voltage phasor at bus j are proportional to $u^{-2}(V_j)$ and $u^{-2}(\theta_j)$, which are computed by using (18) and (19).

IV. Uncertainties in the States Estimated by Using PMU Measurements

The preceding sections describe the methodologies to evaluate the uncertainties associated with the PMU measurements. The next important step is to determine the uncertainties associated with the final states estimated by the WLS estimator. Using (30), the ith estimated state can be expressed as

$$\hat{x}_i=\mathbf{c}_i^{\mathrm{T}}\mathbf{M}\mathbf{z},\quad \forall i=1,\ldots,n \tag{31}$$

where $\mathbf{c}_i\in\Re^n$ is a column vector whose ith element is one and all other elements are zero.

The upper and lower bounds of the estimated state variables can be determined by solving a series of linear optimization problems as shown in the following:

$$\text{Minimize } \mathbf{c}_i^{\mathrm{T}}\mathbf{M}\mathbf{z},\quad \forall i=1,\ldots,n \tag{32}$$
$$\text{Maximize } \mathbf{c}_i^{\mathrm{T}}\mathbf{M}\mathbf{z},\quad \forall i=1,\ldots,n \tag{33}$$
$$\text{subject to } \mathbf{z}_{\text{lower}}\le\mathbf{z}\le\mathbf{z}_{\text{upper}} \tag{34}$$

where (32) and (33) are the sets of objective functions determining the lower and upper bounds of the state variables, respectively.

V. Measurement Uncertainty in the Presence of Conventional Measurements

Although the PMUs are increasingly being used in modern power systems, and it is likely that in the future conventional measurements will be completely replaced by synchronized measurements, the current practice in most systems is to install PMUs in an incremental fashion, in conjunction with conventional measurements. A methodology for estimating the uncertainty interval in the states estimated on the basis of only conventional measurements is described in [16] and [17]. The same procedure can be extended to the measurement set consisting of synchronized as well as conventional measurements.

The upper and lower bounds of the estimated state variables can be determined by solving a series of nonlinear optimization problems as shown in the following:

$$\text{Minimize } \mathbf{c}_i^{\mathrm{T}}\mathbf{x},\quad \forall i=1,\ldots,n \tag{35}$$
$$\text{Maximize } \mathbf{c}_i^{\mathrm{T}}\mathbf{x},\quad \forall i=1,\ldots,n \tag{36}$$
$$\text{subject to } \mathbf{z}'_{\text{lower}}\le\mathbf{z}'(\mathbf{x})\le\mathbf{z}'_{\text{upper}} \tag{37}$$

where $\mathbf{z}'_{\text{lower}}$ and $\mathbf{z}'_{\text{upper}}$ are lower and upper bounds of the measurements, $\mathbf{z}'(\mathbf{x})$ represents the measurement functions expressed in terms of the state variables $\mathbf{x}$.

For conventional measurements such as the power flow and power injection, the measurement functions are the same as the ones used for power flow studies [18], [21]. The current magnitudes and phase angles measured by the PMU can be expressed as a function of the state variables as explained below.

To maintain consistency with the commonly used expressions for conventional measurements, pi-models of transmission lines are assumed while finding the measurement functions for the current magnitude and the phase angle measured by the PMU. Ignoring the shunt admittance, the current phasor from bus i to bus j in Fig. 2 is given by

$$\overline{I}_{ij}=(\overline{V}_i-\overline{V}_j)(g_{ij}+jb_{ij})=C+jD \tag{38}$$

where

$$\begin{aligned}C&=g_{ij}(V_i\cos\theta_i-V_j\cos\theta_j)-b_{ij}(V_i\sin\theta_i-V_j\sin\theta_j)\\ D&=g_{ij}(V_i\sin\theta_i-V_j\sin\theta_j)+b_{ij}(V_i\cos\theta_i-V_j\cos\theta_j).\end{aligned} \tag{39}$$

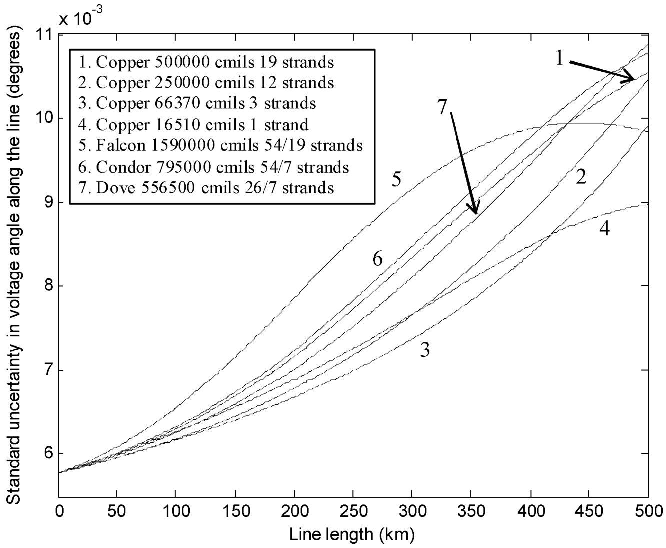

Fig. 3. Variation of standard uncertainty in voltage phase angle for different line lengths.

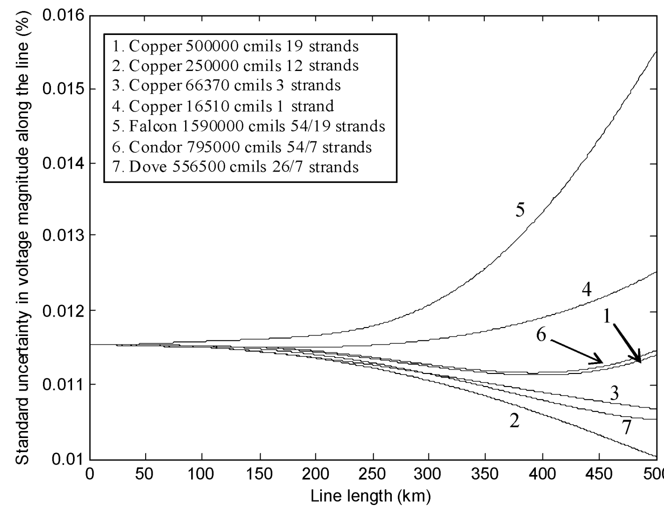

Fig. 4. Variation of standard uncertainty in voltage magnitude for different line lengths.

The magnitude I_{ij} and the phase angle θ_{ij} of the current phasor $\overline{I}_{ij}$ are given by

$$I_{ij} = \sqrt{C^2 + D^2}$$
$$\theta_{ij} = \tan^{-1}(D/C). \quad (40)$$

VI. Case Studies

The case studies presented in this section are organized in two parts. In the first part, the propagation of the PMU measurement uncertainty along transmission lines of varying lengths and types are investigated. In the second part, the uncertainties and the upper and lower bounds for the estimated states are computed for the IEEE 14-bus, IEEE 30-bus, IEEE 57-bus, and IEEE 118-bus test systems [24].

Transmission lines of seven different conductor types, viz., copper conductors (500 000 cmils 19 strands, 250 000 cmils 12 strands, 66 370 cmils 3 strands, and 16 510 cmils 1 strand) and ACSR conductors (Falcon 1 590 000 cmils 54/19 strands, Condor 795 000 cmils 54/7 strands, and Dove 556 500 cmils 26/7 strands) are examined in this study. It is assumed that the conductors are in a horizontal configuration with 4 m spacing between adjacent phases and one conductor per phase. The lines are operating at 60 Hz, and at a 75% loading. Different phase angles for the voltage and current measured by the PMU were assumed and it was observed that the pattern of propagation of uncertainties with line length remains almost the same. In the results shown in this section, the measured voltage and current at the bus where a PMU was installed were assumed to be $1\angle 5^\circ$ p.u. and $0.75\angle -12^\circ$ p.u., respectively, without loss of generality. Fig. 3 shows the propagation of the standard uncertainty in the measurement of the voltage phase angle along the length of the transmission lines of different conductor types. Fig. 4 shows the propagation of the standard uncertainty in the measurement of the voltage magnitude. It is evident from the figures that the propagation of measurement uncertainty depends heavily on the type of conductor. For a WLS state estimator using PMU measurements, weights proportional to the inverse of the square of the associated standard uncertainty can be assigned to the pseudo-measurements of the voltage phasors. This entails assignment of varying weights to the pseudo-measurements by the PMUs, which helps in improving the accuracy of the estimated states.

TABLE I
Optimal Locations of PMUs for the Test Systems

Test system	Optimal PMU locations
IEEE 14-bus	2, 6, 7, 9
IEEE 30-bus	2, 4, 6, 9, 10, 12, 15, 19, 25, 27
IEEE 57-bus	1, 4, 6, 9, 15, 20, 24, 25, 28, 32, 36, 38, 41, 47, 50, 53, 57
IEEE 118-bus	3, 5, 9, 12, 15, 17, 21, 23, 28, 30, 34, 37, 40, 45, 49, 52, 56, 62, 64, 68, 71, 75, 77, 80, 85, 86, 91, 94, 101, 105, 110, 114

The method to compute the uncertainties associated with the PMU measurements is applied in this part of the case study to the IEEE 14-bus, 30-bus, 57-bus, and 118-bus test systems. The optimal locations of the PMUs, to make the systems topologically completely observable so that the total number of PMUs is minimized and the measurement redundancy at the buses is maximized, are shown in Table I [9], [13].

The line length data and the conductor types are not specified for the test systems. However, assuming a specific conductor type and configuration, the line lengths can be computed based on the line impedance data. For the present study, it is assumed that a Dove conductor is used for all the transmission lines in the systems and the conductors are in a horizontal configuration with 4 m spacing between adjacent conductors. The computed line lengths are needed to compute the uncertainties in the pseudo-measurements of the voltage phasors by the PMUs.

Table II shows the standard uncertainties in the magnitude and phase angle of the computed voltage phasors, i.e., the voltage phasors corresponding to the pseudo-measurements. For the PMU buses, the uncertainties are directly computed from the maximum measurement uncertainties specified by the manufacturer (typical values shown in [20]). In this case study, maximum uncertainties in the measurement of voltage

TABLE II
STANDARD UNCERTAINTY IN THE PSEUDO-MEASUREMENTS OF PHASE ANGLES AND MAGNITUDES OF THE VOLTAGE PHASORS FOR THE IEEE 14-BUS TEST SYSTEM

PMU bus	Measurement bus	$u(\theta)$ (degrees)	$u(V)$ (%)	Maximum TVE
2	1	0.005852	0.012085	0.004917
	3	0.006132	0.012067	0.003733
	4	0.005946	0.012046	0.001272
	5	0.005910	0.012035	0.001575
6	5	0.006093	0.012296	0.001927
	11	0.005829	0.012292	0.001068
	12	0.005833	0.012250	0.001985
	13	0.005853	0.012331	0.001035
7	4	0.005746	0.012204	0.001016
	8	0.005624	0.012222	0.001014
9	4	0.005894	0.011706	0.001532
	10	0.005797	0.012182	0.001015
	14	0.005861	0.012079	0.001014

and current magnitude are 0.02% and 0.03% of the reading, respectively, and the maximum error in the measurement of phase angle is 0.01 degrees.

The measurement uncertainties are used to construct the covariance matrix $\mathbf{R}$ for the test systems, as shown in (29). This provides the basis for weighing the measurements. For instance, the measurement having greater uncertainty is assigned less weight compared to the one having a smaller uncertainty. The weights assigned to the measurements are proportional to the inverse of the square of the measurement uncertainties.

The maximum possible total vector error (TVE) in the measurement of voltage phasors, which is the objective function in the optimization problem shown in (22), is found in this study by using Monte Carlo simulation. The measurements are assumed to have uniform probability distribution within the range specified in (23). For each measurement, 10^6 samples are taken randomly from the specified range. These samples are then used to evaluate the TVE for the corresponding measurement. The maximum TVE for a voltage phasor is the maximum of the 10^6 number of evaluations. The last column in Table II shows the maximum TVEs for the pseudo-measurement of voltage phasors for the 14-bus test system.

Figs. 5–7 show the uncertainties associated with the pseudo-measurements for the IEEE 30-, 57- and 118-bus test systems. The order in which the PMU buses are selected to depict the measurement uncertainties is the same as in Table I for all the test systems. The order of selecting non-PMU buses connected to a PMU bus corresponds to the order of line numbers given in system data files in [24]. For example, from Table I, the first PMU location for the 30-bus system is bus-2, which is connected to the buses 1, 4, 5, and 6 via lines that are numbered as 1, 3, 4, and 5 in [24]. The first pair of data points in Fig. 5 therefore corresponds to bus-1, the second to bus-4, and so on. The variation in the standard uncertainties of the pseudo-measurements of voltage phase angles and magnitudes suggests the use of varying weights for the measurements in the WLS formulation for state estimation.

Table III shows the standard deviations (as a percentage of the mean) of the standard uncertainties in the pseudo-measurements for the test systems. To simplify the study, only a Dove

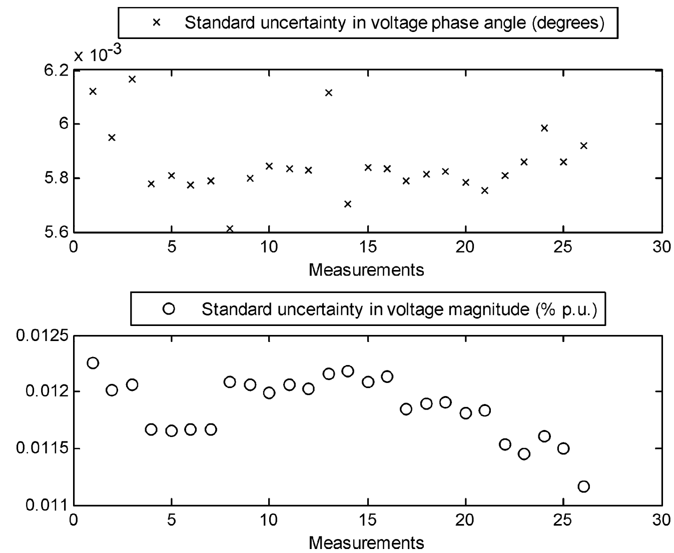

Fig. 5. Standard uncertainties in the pseudo-measurements of voltage phase angles and magnitudes for the IEEE 30-bus test system.

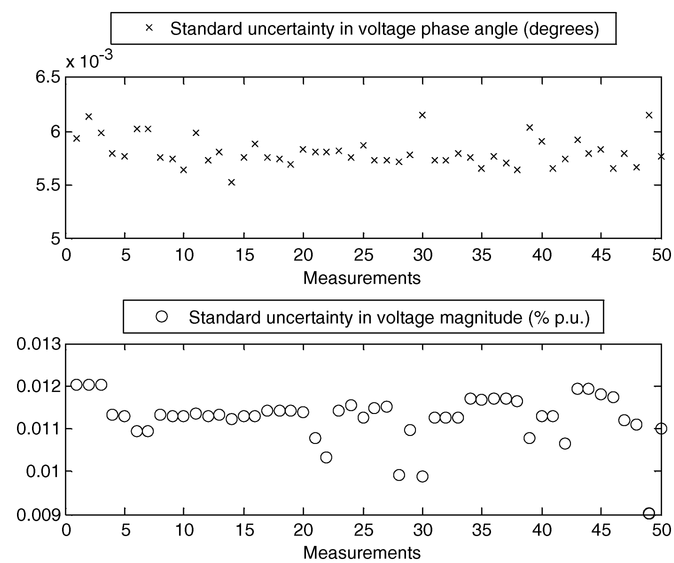

Fig. 6. Standard uncertainties in the pseudo-measurements of voltage phase angles and magnitudes for the IEEE 57-bus test system.

conductor is assumed for the whole system. In actual power systems, different types of conductors exist, which is likely to result in a greater variation in the uncertainties, and hence in the weights associated with the pseudo-measurements. Figs. 8–10 depict the maximum TVEs corresponding to the pseudo-measurements of voltage phasors for the 30-, 57-, and 118-bus test systems. Although for the test systems studied in this section the maximum TVEs for the pseudo-measurements lie within 1% compliance limit, in general, there are two occasions for the 57-bus system, as evident from Fig. 9, where the maximum TVE is greater than 1%. Depending on the specified compliance level, the proposed methodology therefore provides a basis for eliminating the pseudo-measurements from the measurement set, for which the TVE is greater than the specified minimum value.

The next step is to find the uncertainties in the states estimated by the WLS state estimator using PMU measurements.

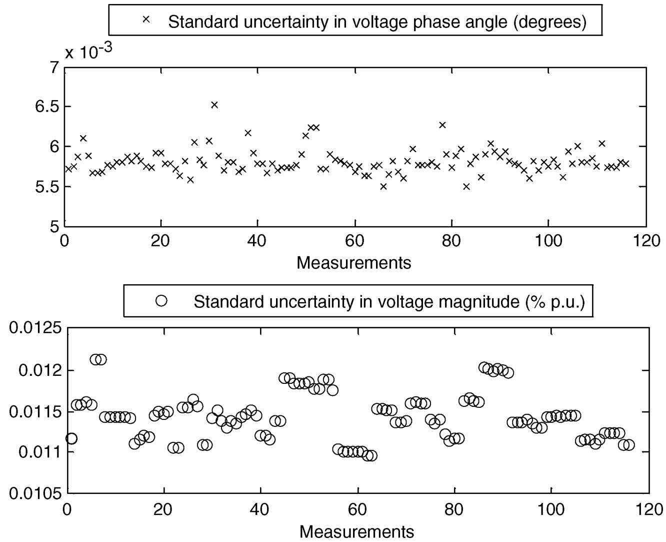

Fig. 7. Standard uncertainties in the pseudo-measurements of voltage phase angles and magnitudes for the IEEE 118-bus test system.

TABLE III
STANDARD DEVIATION OF THE STANDARD UNCERTAINTIES FOR PSEUDO-MEASUREMENTS FOR THE TEST SYSTEMS

Test system	**Standard deviation (as a percentage of the mean)**	
	Standard uncertainty in voltage phase angle (%)	**Standard uncertainty in voltage magnitude (%)**
IEEE 14-bus	2.25	1.32
IEEE 30-bus	1.89	2.29
IEEE 57-bus	2.72	5.48
IEEE 118-bus	2.65	2.30

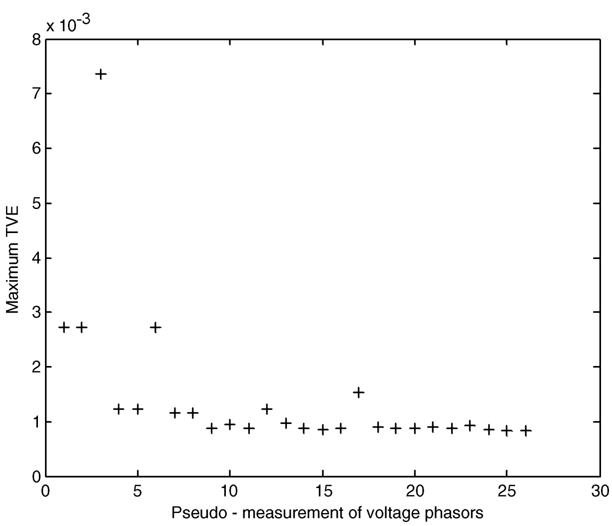

Fig. 8. Maximum values of the total vector error (TVE) for the pseudo-measurements of voltage phasors for the IEEE 30-bus test system.

The weights assigned to the measurements in WLS state estimation are proportional to the inverse of the square of the measurement uncertainties. The upper and lower bounds in the estimated states as a result of the uncertainty in the measurement are obtained by solving the linear optimization problems formulated in (32) and (33). The TOMLAB optimization toolbox is used to solve the linear programming problems [25]. Table IV shows

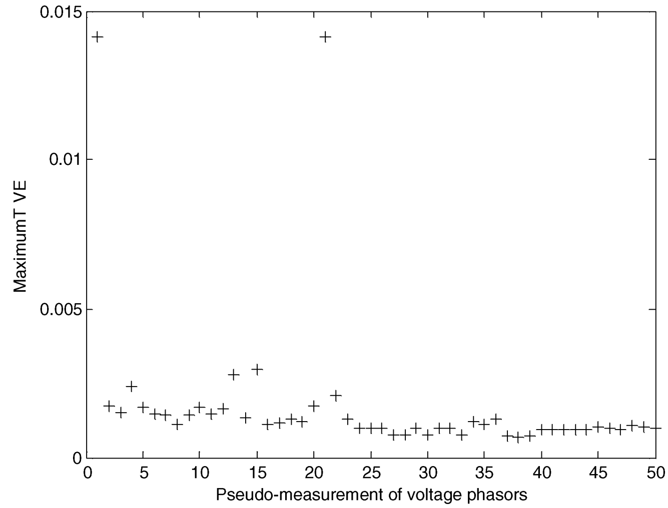

Fig. 9. Maximum values of the total vector error (TVE) for the pseudo-measurements of voltage phasors for the IEEE 57-bus test system.

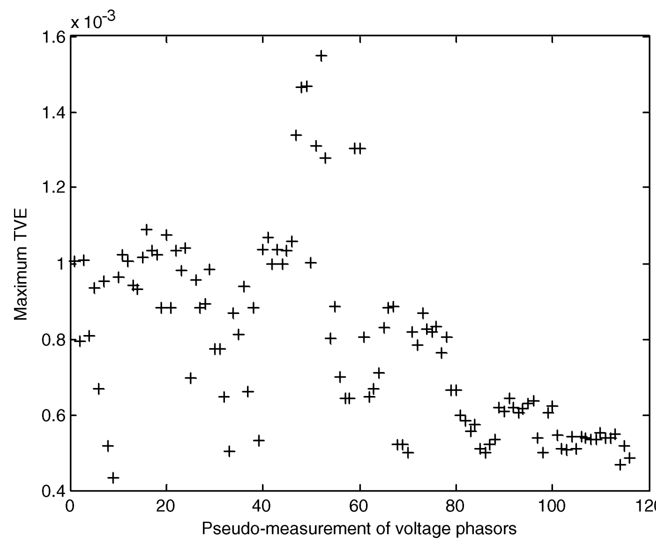

Fig. 10. Maximum values of the total vector error (TVE) for the pseudo-measurements of voltage phasors for the IEEE 118-bus test system.

the estimated values of the voltage phase angles and magnitudes for the 14-bus system, along with the upper and lower limits of the estimated values. Table V shows similar simulation results for the IEEE 30-bus test system.

The proposed method to determine the uncertainty associated with the PMU measurements and the effect of the uncertainty on the final estimated states is also applied on the IEEE 57-bus and IEEE 118-bus test systems. For these two test systems, Figs. 11 and 12 graphically demonstrate the maximum uncertainty associated with the estimated states, which is obtained by determining the absolute values of the differences between the upper and lower limits of the estimated states.

It is to be noted that each of the upper and lower limits of the estimated states are obtained by solving a separate optimization problem as described in (32) and (33). The uncertainties in measurements while evaluating a particular limit value are such that the estimated state acquires the minimum or the maximum

TABLE IV
ESTIMATED VALUES AND THE UPPER AND LOWER LIMITS OF THE VOLTAGE PHASE ANGLES AND MAGNITUDES FOR THE 14-BUS TEST SYSTEM

Bus No.	Voltage phase angle (degrees)			Voltage magnitude (p.u.)		
	Upper limit	Estimated value	Lower limit	Upper limit	Estimated value	Lower limit
1	0.0101	0	-0.0101	1.06020	1.06000	1.05979
2	-4.9700	-4.9800	-4.9899	1.04520	1.04500	1.04479
3	-12.7093	-12.7200	-12.7306	1.01020	1.01000	1.00979
4	-10.3198	-10.3299	-10.3401	1.01920	1.01900	1.01879
5	-8.7696	-8.7799	-8.7903	1.02021	1.02000	1.01978
6	-14.2100	-14.2200	-14.2299	1.07021	1.07000	1.06978
7	-13.3600	-13.3700	-13.3799	1.06221	1.06200	1.06178
8	-13.3502	-13.3599	-13.3697	1.09021	1.09000	1.08978
9	-14.9300	-14.9400	-14.9499	1.05621	1.05600	1.05578
10	-15.0899	-15.1000	-15.1100	1.05121	1.05100	1.05078
11	-14.7799	-14.7899	-14.8000	1.05721	1.05700	1.05678
12	-15.0599	-15.0699	-15.0800	1.05521	1.05500	1.05478
13	-15.1498	-15.1599	-15.1701	1.05021	1.05000	1.04978
14	-16.0298	-16.0399	-16.0501	1.03620	1.03600	1.03579

TABLE V
ESTIMATED VALUES AND THE UPPER AND LOWER LIMITS OF THE VOLTAGE PHASE ANGLES AND MAGNITUDES FOR THE 30-BUS TEST SYSTEM

Bus No.	Voltage phase angle (degrees)			Voltage magnitude (p.u.)		
	Upper limit	Estimated value	Lower limit	Upper limit	Estimated value	Lower limit
1	0.0099	0	-0.0099	1.06021	1.06000	1.05978
2	-5.3400	-5.3500	-5.3599	1.04334	1.04314	1.04293
3	-7.5194	-7.5300	-7.5405	1.02100	1.02079	1.02057
4	-9.2697	-9.2800	-9.2902	1.01199	1.01179	1.01158
5	-14.1593	-14.1699	-14.1806	1.01021	1.01001	1.00980
6	-11.0500	-11.0600	-11.0699	1.01048	1.01028	1.01007
7	-12.8499	-12.8600	-12.8700	1.00259	1.00239	1.00218
8	-11.8000	-11.8099	-11.8199	1.01021	1.01001	1.00980
9	-14.1000	-14.1100	-14.1199	1.05113	1.05093	1.05072
10	-15.6900	-15.7000	-15.7099	1.04535	1.04515	1.04494
11	-14.1002	-14.1100	-14.1197	1.08221	1.08201	1.08180
12	-14.9300	-14.9400	-14.9499	1.05735	1.05714	1.05692
13	-14.9301	-14.9400	-14.9498	1.07122	1.07101	1.07079
14	-15.8199	-15.8299	-15.8400	1.04250	1.04230	1.04209
15	-15.9200	-15.9300	-15.9399	1.03790	1.03770	1.03749
16	-15.5199	-15.5299	-15.5400	1.04462	1.04441	1.04419
17	-15.8499	-15.8600	-15.8700	1.04012	1.03992	1.03971
18	-16.5299	-16.5400	-16.5500	1.02837	1.02817	1.02796
19	-16.7000	-16.7099	-16.7199	1.02587	1.02567	1.02546
20	-16.5099	-16.5199	-16.5300	1.02996	1.02976	1.02955
21	-16.1299	-16.1400	-16.1500	1.03295	1.03275	1.03254
22	-16.1199	-16.1299	-16.1400	1.03348	1.03328	1.03307
23	-16.3099	-16.3200	-16.3300	1.02740	1.02720	1.02699
24	-16.4799	-16.4900	-16.5000	1.02179	1.02160	1.02140
25	-16.0600	-16.0700	-16.0799	1.01756	1.01736	1.01715
26	-16.4798	-16.4900	-16.5001	0.99987	0.99968	0.99948
27	-15.5300	-15.5400	-15.5499	1.02347	1.02327	1.02306
28	-11.6798	-11.6899	-11.7001	1.00703	1.00683	1.00662
29	-16.7598	-16.7700	-16.7801	1.00362	1.00343	1.00323
30	-17.6397	-17.6499	-17.6602	0.99215	0.99196	0.99176

possible value. Therefore, the distribution of measurement uncertainties corresponding to each of the limit values may be different.

The case studies discussed above consider the minimum number of PMUs that can make the test systems observable. It is possible to include a desired minimum measurement redundancy criterion in the PMU placement problem [12], [13]. By ensuring a measurement redundancy of at least one at all the

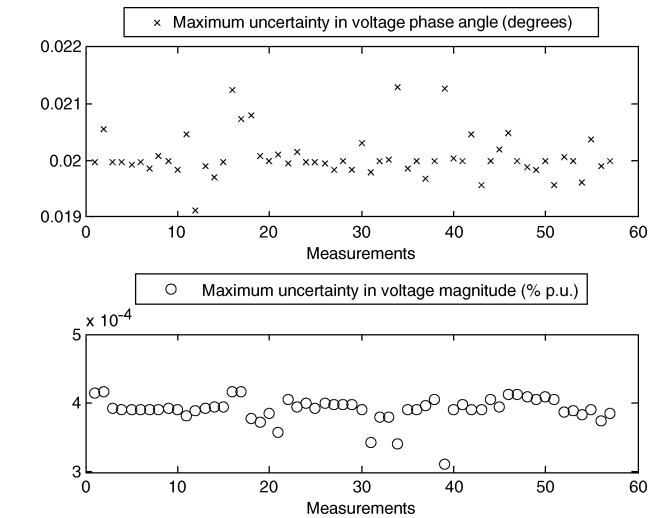

Fig. 11. Maximum uncertainties in the estimated values of the voltage phase angles and the magnitudes for the IEEE 57-bus test system.

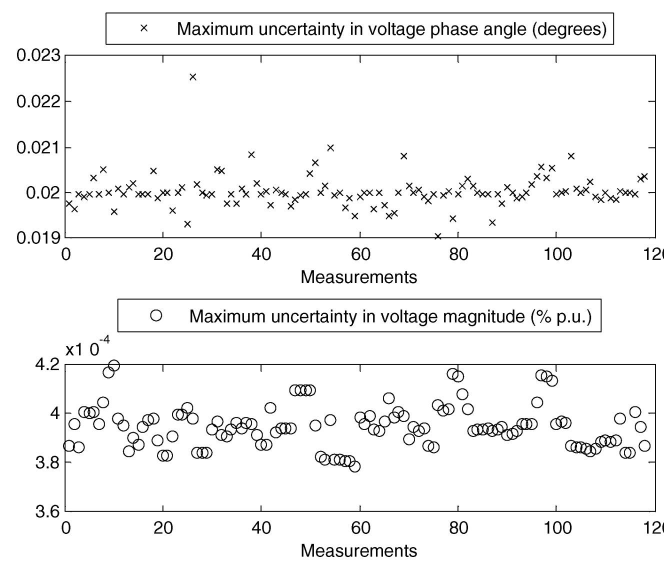

Fig. 12. Maximum uncertainties in the estimated values of the voltage phase angles and the magnitudes for the IEEE 118-bus test system.

buses, the occurrence of critical measurements can be avoided, thereby helping in detecting bad data in the measurement set [26].

The IEEE 14-bus test system is employed as an example of finding the upper and lower bounds of the estimated states in the case of having both synchronized and conventional measurements. In this system, it is assumed (without loss of generality) that nine injection measurements and six power flow measurements are available, as shown in Fig. 13. In order to render the system completely observable, two PMUs are required (see [13] for related theory and how to determine PMU locations in the presence of conventional measurements).

Table VI shows the upper and lower bounds of the estimated states for the measurement configuration shown in Fig. 13. The maximum uncertainty for the conventional measurements is assumed to be 3% of the reading [16].

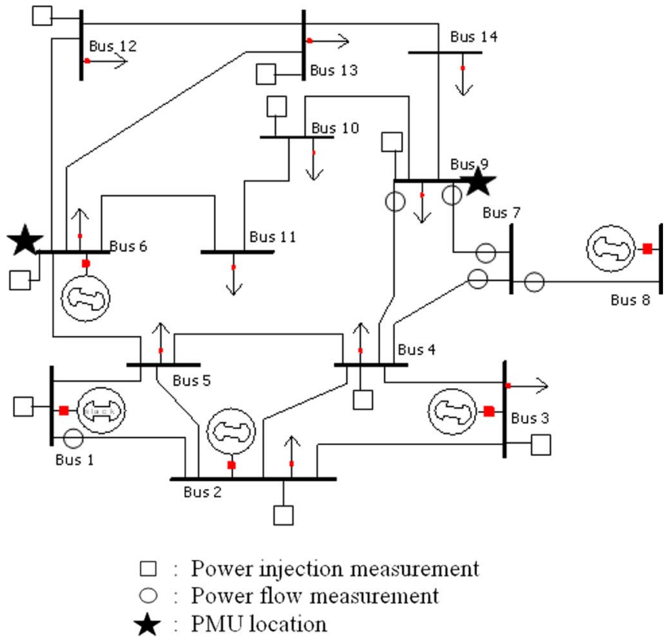

Fig. 13. IEEE 14-bus test system with conventional measurements and PMUs.

TABLE VI
UPPER AND LOWER LIMITS OF THE VOLTAGE PHASE ANGLES AND MAGNITUDES FOR THE 14-BUS TEST SYSTEM IN THE PRESENCE OF CONVENTIONAL MEASUREMENTS

Bus No.	Voltage phase angle (degrees)		Voltage magnitude (p.u.)	
	Upper limit	Lower limit	Upper limit	Lower limit
1	0	0	1.0718	1.0135
2	-4.4830	-5.2470	1.0724	0.9828
3	-11.4962	-12.8553	1.0219	0.9876
4	-9.4330	-11.1747	1.0708	0.9758
5	-8.0754	-9.0058	1.0230	0.9383
6	-13.8457	-14.4794	1.1319	1.0177
7	-12.5976	-14.5353	1.1201	0.9597
8	-12.5302	-14.5011	1.1580	1.0367
9	-14.8292	-15.5432	1.1603	1.0172
10	-14.7352	-15.3751	1.1347	0.9550
11	-13.3909	-16.1230	1.1288	1.0216
12	-13.7125	-15.5777	1.1240	1.0437
13	-14.5696	-16.3434	1.1449	0.9749
14	-15.8311	-16.1976	1.0565	0.9636

VII. CONCLUSIONS

The uncertainties associated with the direct and pseudo-measurements obtained by using PMUs are evaluated in this paper. A methodology is proposed to evaluate the uncertainties in the pseudo-measurements by using the classical uncertainty propagation theory. A basis for weighing PMU measurements in a WLS state estimation is provided by investigating the propagation of the measurement uncertainty for different line lengths and conductors. The TVEs for the voltage phasors computed by using PMU measurements are also determined to verify the compliance of the pseudo-measurements with the standards. Considering the measurement uncertainties, a linear programming based methodology is proposed to determine the upper and lower limits of the states estimated by using the PMU measurements. The proposed methodologies are demonstrated on IEEE 14-, 30-, 57-, and 118-bus test systems. The methodology to determine the uncertainties in the estimated states when conventional measurements are present along with PMU measurements is also presented in the paper and applied on a test system.

REFERENCES

[1] D. Novosel, V. Madani, B. Bhargava, K. Vu, and J. Cole, "Dawn of the grid synchronization," *IEEE Power Energy Mag.*, vol. 6, no. 1, pp. 49–60, Jan./Feb. 2008.
[2] Real Time Dynamics Monitoring System. [Online]. Available: http://www.phasor-rtdms.com.
[3] J. Zhu, A. Abur, M. J. Rice, G. T. Heydt, and S. Meliopoulos, Enhanced State Estimators, PSERC, Nov. 2006, Fin. Proj. Rep.
[4] *IEEE Standard for Synchrophasors for Power Systems*, IEEE Std. C37.118TM-2005, IEEE Power Engineering Society.
[5] D. Novosel *et al.*, Performance Requirements: Part II, Eastern Interconnection Phasor Project, Jun. 2006.
[6] T. L. Baldwin, L. Mili, M. B. Boisen, Jr., and R. Adapa, "Power system observability with minimal phasor measurement placement," *IEEE Trans. Power Syst.*, vol. 8, no. 2, pp. 707–715, May 1993.
[7] R. F. Nuqui and A. G. Phadke, "Phasor measurement unit placement techniques for complete and incomplete observability," *IEEE Trans. Power Del.*, vol. 20, no. 4, pp. 2381–2388, Oct. 2005.
[8] B. Milosevic and M. Begovic, "Nondominated sorting genetic algorithm for optimal phasor measurement placement," *IEEE Trans. Power Syst.*, vol. 18, no. 1, pp. 69–75, Feb. 2003.
[9] B. Xu and A. Abur, Optimal Placement of Phasor Measurement Units for State Estimation, PSERC, Oct. 2005, Fin. Proj. Rep.
[10] B. Xu and A. Abur, "Observability analysis and measurement placement for systems with PMUs," in *Proc. IEEE PES Power Systems Conf. Expo.*, Oct. 2004, pp. 943–946.
[11] C. Rakpenthai, S. Premrudeepreechacharn, S. Uatrongjit, and N. R. Watson, "An optimal PMU placement method against measurement loss and branch outage," *IEEE Trans. Power Del.*, vol. 22, no. 1, pp. 101–107, Jan. 2005.
[12] S. Chakrabarti and E. Kyriakides, "Optimal placement of phasor measurement units for power system observability," *IEEE Trans. Power Syst.*, vol. 23, no. 3, pp. 1433–1440, Aug. 2008.
[13] S. Chakrabarti, E. Kyriakides, and D. G. Eliades, "Placement of synchronized measurements for power system observability," *IEEE Trans. Power Del.*, vol. 24, no. 1, pp. 12–19, Jan. 2009.
[14] S. Chakrabarti, D. Eliades, E. Kyriakides, and M. Albu, "Measurement uncertainty considerations in optimal sensor deployment for state estimation," in *Proc. IEEE Symp. Intelligent Signal Processing*, Alcala de Henares, Spain, Oct. 2007.
[15] S. Chakrabarti, E. Kyriakides, and M. Albu, "Uncertainty in power system state variables obtained through synchronized measurements," *IEEE Trans. Instrum. Meas.*, to be published.
[16] A. K. Al-Othman and M. R. Irving, "Uncertainty modeling in power system state estimation," *Proc. Inst. Elect. Eng., Gen., Transm., Distrib.*, vol. 152, no. 2, pp. 233–239, Mar. 2005.
[17] A. K. Al-Othman and M. R. Irving, "A comparative study of two methods for uncertainty analysis in power system state estimation," *IEEE Trans. Power Syst.*, vol. 20, no. 2, pp. 1181–1182, May 2005.
[18] J. D. Glover and M. S. Sarma, *Power System Analysis and Design*, 3rd ed. Pacific Grove, CA: Thomson Learning, 2002.
[19] ISO-IEC-OIML-BIPM: Guide to the Expression of Uncertainty in Measurement, 1992.
[20] *"Model 1133A GPS-Synchronized Power Quality/Revenue Standard, Operation Manual,"* Arbiter Systems, Paso Robles, CA.
[21] A. Abur and A. G. Exposito, *Power System State Estimation: Theory and Implementation*. New York: Mercel Dekker, 2004.
[22] V. Terzija, "SMT based real time state estimation," *Tutorial on Wide Area Monitoring, Protection, and Control*. Manchester, U.K., Jun. 12–14, 2007.
[23] X. Bei, Y. J. Yoon, and A. Abur, "Optimal placement and utilization of phasor measurements for state estimation," in *Proc. 15th Power Systems Computation Conf.*, Liege, Belgium, Aug. 2005.
[24] R. Christie, Aug. 1999, Power System Test Archive. [Online]. Available: http://www.ee.washington.edu/research/pstca.
[25] TOMLAB, Release 5.7.0, Tomlab Optimization, 2006.
[26] J. Chen and A. Abur, "Placement of PMUs to enable bad data detection in state estimation," *IEEE Trans. Power Syst.*, vol. 21, no. 4, pp. 1608–1615, Nov. 2006.

Saikat Chakrabarti (S'06–M'07) received the B.E. degree in 1997 from the National Institute of Technology, Durgapur, India, the M.E. degree in 2000 from Jadavpur University, Calcutta, India, and the Ph.D. degree in 2006 from Memorial University of Newfoundland, St. John's, NF, Canada, all in electrical engineering.

He worked with ABB Ltd., India, from 1997 to 1998 and with the Bhabha Atomic Research Center, India, from 2000 to 2002. From 2006 to 2008, he worked as a postdoctoral fellow in the Department of Electrical and Computer Engineering, University of Cyprus. Currently, he is appointed as a Lecturer in the School of Engineering Systems, Queensland University of Technology, Brisbane, Australia. His research interests include power system dynamics and stability, state estimation, power electronics, and renewable energy systems.

Elias Kyriakides (S'00–M'04) is from Nicosia, Cyprus. He received the B.Sc. degree from the Illinois Institute of Technology, Chicago, in 2000, and the M.Sc. and Ph.D. degrees from Arizona State University, Tempe, in 2001 and 2003, respectively, all in electrical engineering.

He is a founding member of the KIOS Research Center for Intelligent Systems and Networks and a Lecturer in the Department of Electrical and Computer Engineering at the University of Cyprus. His research interests include synchronized measurements in power systems, security and reliability of the power system network, optimization of power system operation techniques, modeling of electric machines, and renewable energy sources.